ISSN (Print) : 0974-6846
Indian Journal of Science and Technology, *Vol 9(17), DOI: 10.17485/ijst/2016/v9i17/92969, May 2016* ISSN (Online) : 0974-5645

Application of Multiple Signal Classification Algorithm on GPS TEC for Earthquakes

S. K. Baji*, R. Revathi, S. Lakshminarayana, S. Koteswara Rao and K. S. Ramesh

K L University, Green fields, Vaddeswaram - 522502, Andhra Pradesh, India; bajishaik54@gmail.com, revathimouni@gmail.com, dr.ramesh@kluniversity.in, skrao@kluniversity.in

Abstract

Background/Objectives: The major objective of our work is to identify the precursors of earthquakes and analysed the precursors in ionosphere prior to the occurrence of earthquake using Global Positioning System Total Electronic Content (GPSTEC). **Methods/Statistical Analysis:** In this work Multiple Signal Classification algorithm (MUSIC) is explored. MUSIC estimates the frequency content of a signal or autocorrelation matrix using a Eigen space method. **Findings:** It is clearly observed that there is a significant raise in energy of the ionosphere on the day of earthquake occurrence. **Application/ Improvement:** If the quality data is available before and after the occurrence of earthquake also, then it may be possible to develop the early warning system for earthquakes.

Keywords: Earthquakes, GPSTEC, Ionosphere, Multiple Signal Classification (MUSIC), Seismo-ionospheric Perturbations

1. Introduction

DEMETER, a French micro satellite has observed that its signals are affected by the electrostatic and magnetic field anomalies before the occurrence of earthquakes[1,2,3]. The electric and magnetic field anomalies lead to seismogenic perturbations in ionosphere. These perturbations have been statistically established by many researchers[4].

The epicentre area of earthquake occurrence is prevalent with mechanical transformations and also with dominant active geochemical processes. These process emanate radon, noble and greenhouse gasses and a large amount of metal aerosols such as Cu, Fe, Ni and Zn into the atmosphere near the ground[3,5]. The radon released from the earth surface ionizes the gases near the ground. The ionization of the lower atmosphere leads to the formation vertical electrical field[6]. The existing Lithosphere-Atmosphere-Ionosphere coupling mechanism is consistent with these changes[7].

The ground based Global Positioning Systems (GPS) receivers, receive the signals travelling through the ionosphere. The ionosphere causes group and phase delay in the GPS signals passing through it. The phase and group delay of the GPS signals is equal in magnitude but opposite in phase. The phase delay in seconds is measured as the integral value of the electron density in the line of sight between the satellite and the receiver. This is called as the slant total electron content (STEC).The phase delay of the GPS signals measured in meters is called the pseudo range. The satellite position in the orbit is calculated by the navigation information transmitted by GPS satellites. Ground based GPS receiver matches the pseudorandom number (PRN) code transmitted by GPS satellites and calculates the time delay introduced in the transmitted signal using "time of arrival".

The pseudo range in meters for a single frequency GPS receiver 'ρ_{L_1}', is given by

$$\rho_{L_1} = (40.3*\text{STEC})/f_{L_1}^{\ 2} \quad (1)$$

For a dual frequency GPS receiver, it is given by

* *Author for correspondence*

$$\rho_{L_1} - \rho_{L_2} = (40.3*\text{STEC})*[(1/f_{L_1}^{\ 2}) - (1/f_{L_2}^{\ 2})] \quad (2)$$

where 'f_{L_1}', and 'f_{L_2}', frequencies correspond to GPS 'L_1' and 'L_2', signals. For a dual frequency GPS receiver STEC is given by

$$\text{STEC} = \left[\frac{(\rho_{L_1} - \rho_{L_2})}{40.3}\right] * \left[\frac{f_{L_1}^{\ 2} * f_{L_2}^{\ 2}}{f_{L_1}^{\ 2} - f_{L_2}^{\ 2}}\right] \quad (3)$$

As the satellite is moving, the STEC values are recorded by the GPS receiver. These STEC values are converted to vertical total electron content (VTEC) by taking the cosine of the difference between 90° and the satellite zenith angle at a height of 350km. It is given by

$$\text{VTEC}=\text{STEC}*(\text{Cos}(\chi)) \quad (4)$$

The advantages of using data of a single ground based GPS receiver are 1.It data does not contain modelling errors and 2. It has uniform sampling period over the entire data record. This aids in the implementation of the Spectral estimation techniques on GPS TEC[8].

So far, wavelets, integrated wavelet transforms and principal component analysis (PCA) are applied on the global TEC data sets (GIM etc.) to identify earthquake precursors. These studies provide an evidence for the increasing TEC from 5 to 10 days before the occurrence of the earthquake[9,10,11].

Spectral estimation methods provide a good statistical and highly reliable estimation of the signal. In this paper Multiple signal classification algorithm (MUSIC) is implemented on the disturbed VTEC data of the earthquake day. The high resolution analysis of this method enables us to understand energy perturbation in ionosphere due to the impending earthquake.

2. Event Considered

Earthquake has occurred on 15th January 2014 in Java, Indonesia (6.575°S, 106.334°E) at 9:26 hours Universal Time Coordinate (UTC), i.e. at 14:26 hours Local Time Coordinate (LTC) with a depth of 125km. The magnitude of the earthquake is 4.5 on Ritcher Scale. This event is considered for analysis. The boundary of the Australian Pacific plate and the east coast of Pupa New Guinea are dominated by the general northward subduction of the Australian plate. The location map of the earthquake is shown in the Figure 1. The location map of the earthquake is taken from http://earthquaketrack.com/quakes/2014-01-15-09-26-11-utc-4-5-125

Figure 1. Location map of earthquake occurrence.

3. Data

GPS VTEC is provided by the International Global Navigation Satellite systems (IGS). The VTEC values are collected from the IGS station named BAKO, situated at Bakosurtanal, West Java, Indonesia (6.490°S, 106.850°E). The earthquake has occurred on 15th day of year 2014. It is observed that the VTEC data of satellite PRN number 18 is disturbed on 14th,15th (earthquake day) and 16th of January 2014.The VTEC data of three days taking the earthquake day as the middle is subjected to the analysis.

The VTEC plot of PRN number 18 for three days is shown in Figure 2, Figure 3, and Figure 4 respectively. It is observed that VTEC was disturbed for three hours before the occurrence of the earthquake. The ray path of the satellite PRN number 18 with respect to time is given in Figure 5.

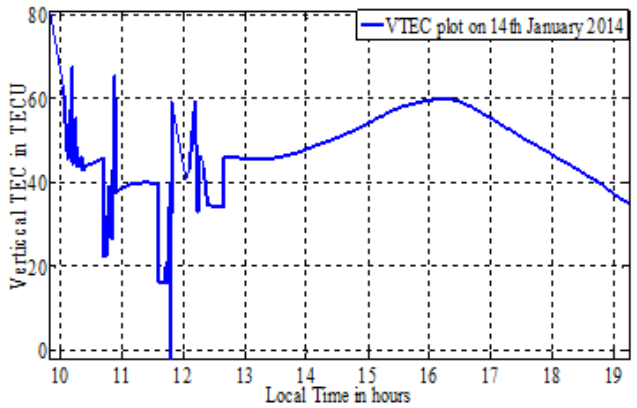

Figure 2. VTEC plot of PRN 18 on 14th January 2014.

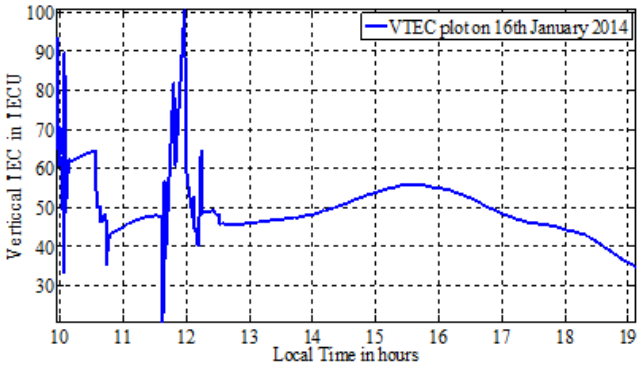

Figure 3. VTEC plot of PRN 18 on 15th January 2014.

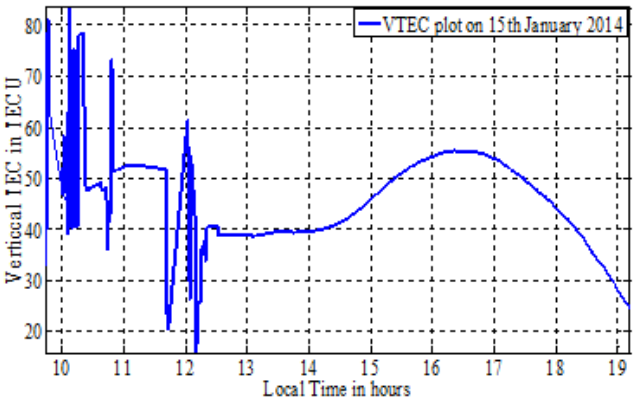

Figure 4. VTEC plot of PRN 18 on 16th January.

This IGS station BAKO is situated at 58 km away from the epicenter of the earthquake. It is clearly observed from Figure 5 that the satellite is passing over the earthquake area at the time of the occurrence of perturbation in VTEC. The undisturbed data is considered upto 15 hours LTC as the VTEC data after this time is the representation of the post sunset phenomenon at this low latitude station.

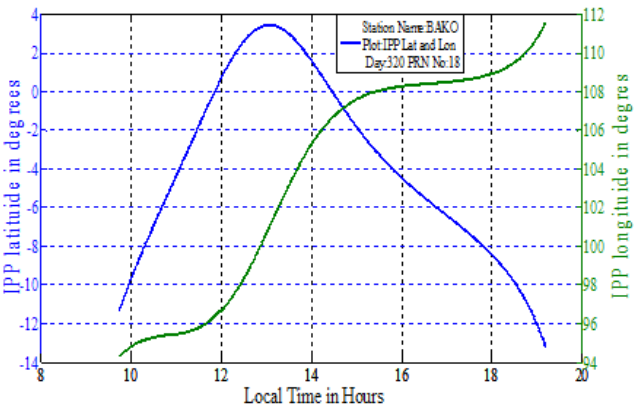

Figure 5. Satellite ray path of PRN 18.

4. Methodology

There are many statistical signal processing algorithms available to find out the disturbances in the signals [12–15]. In this research work multiple signal classification algorithm (MUSIC) is explored[16]. The power spectral density of the disturbed VTEC and undisturbed VTEC is estimated by using MUSIC algorithm. In the MUSIC, eigen space determines the auto correlation matrix or frequency content of the signal. In this algorithm an assumption is taken that the signal x(n) consists of 'p', complex exponentials in the presence of Gaussian white noise. Given an auto correlation matrix 'R_x', if the eigen values are sorted in decreasing order, the eigenvectors corresponding to the 'p', largest eigen values (i.e. direction of largest variability) span the signal subspace. Noise is represented by the remaining M – p eigen vectors which span the orthogonal space. MUSIC is indistinguishable to pisarenko harmonic decomposition for M = p+1. To get the better performance of pisarenko estimator, averaging is employed. Music algorithm was developed for a synthetic signal x(n) consisting of four frequencies given as

$$x(n) = u(n) + v(n)$$

$$u(n) = 5(\exp(j*0.5n) + \exp(j(0.n + \varphi_1)) + \exp(j(0.8n + \varphi_2)) + \exp(j(0.9n + \varphi_3)))$$

with a phase shift of $\phi_1 = 20*\pi/180$, $\phi_2 = 20*\pi/180$, $\phi_3 = 20*\pi/180$ and n = 64, v(n) is zero mean unit variance white noise. The simulated results are shown Figure 6.

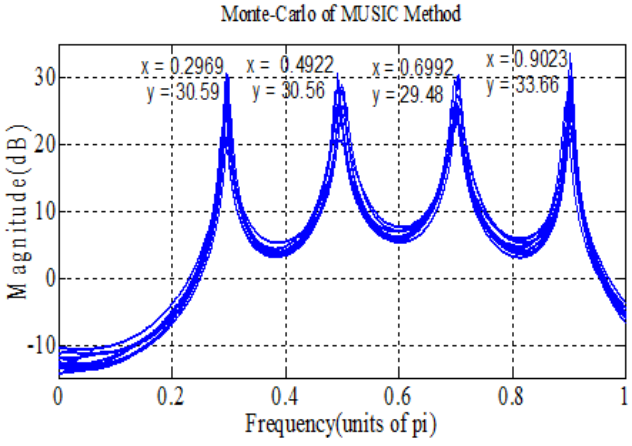

Figure 6. Mont - Carlo simulation of synthetic signal using MUSIC method.

Since the results are good for synthetic signal, MUSIC algorithm is implemented on VTEC data of three days taking the earthquake day as the middle one.

5. Results

VTEC data of PRN 18 for the three days is analyzed for earthquake signatures. The detrended disturbed and undisturbed VTEC data of the three days were subjected to analysis. The detrended disturbed and undisturbed VTEC plots of the three days are as shown in Figure 7 and Figure 8. The PSDs of disturbed VTEC for the three days are shown in Figure 9, Figure 10 and Figure 11.

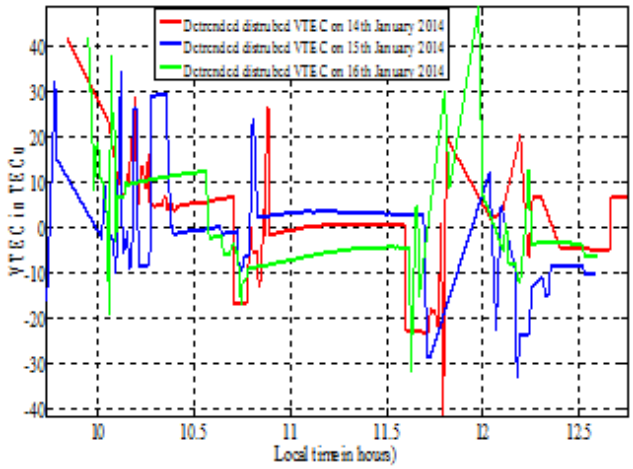

Figure 7. Detrended disturbed VTEC for 14th, 15th, and 16th January 2014.

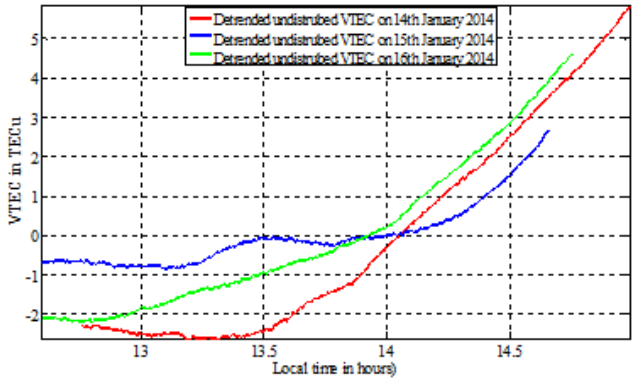

Figure 8. Detrended undisturbed VTEC for 14,5th and 16th January 2014.

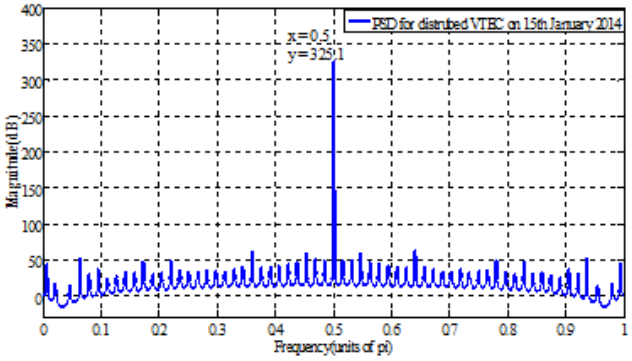

Figure 9. DPSD for detrended disturbed VTEC of 14th January 2014 for PRN 18.

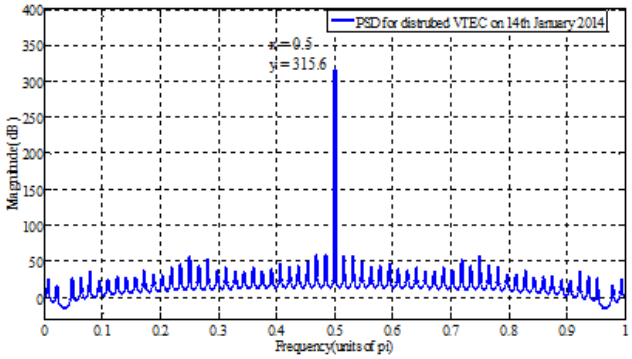

Figure 10. PSD for detrended disturbed VTEC of 15th January 2014 for PRN 18.

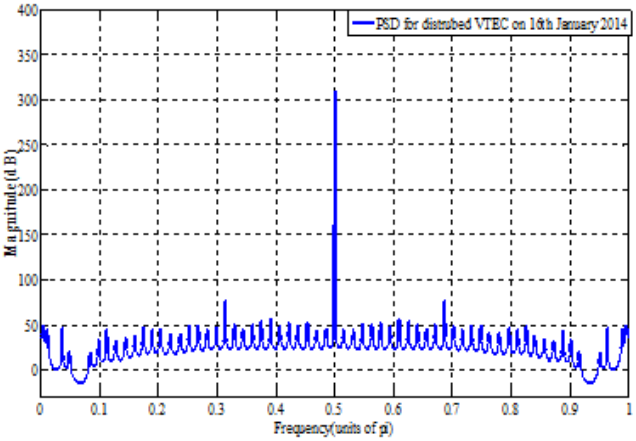

Figure 11. PPSD for detrended disturbed VTEC of 16th January 2014 for PRN 18.

The PSDs for the undisturbed VTEC data are shown in Figure 12, Figure 13, Figure 14. It can be clearly observed

that the PSD of the disturbed VTEC on the earthquake day (15th January 2014) is high when compared to the PSD of the 14th and 16th January 2014. It is also clearly observed that the PSDs of disturbed VTEC are around 10dB more than the PSDs of undisturbed VTEC on the three consecutive days taking the earthquake day as the middle one. The results are tabulated in Table 1.

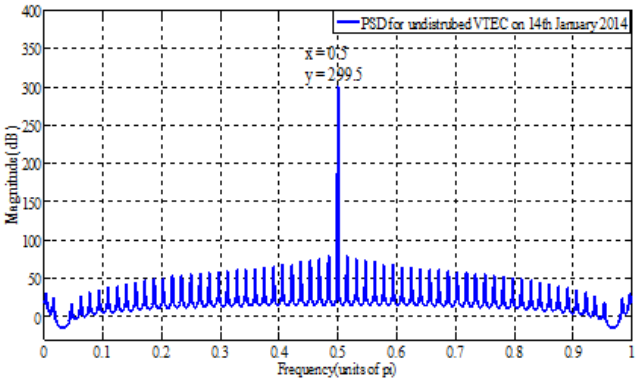

Figure 12. PSD for detrended undisturbed VTEC of 14th January 2014 for PRN 18.

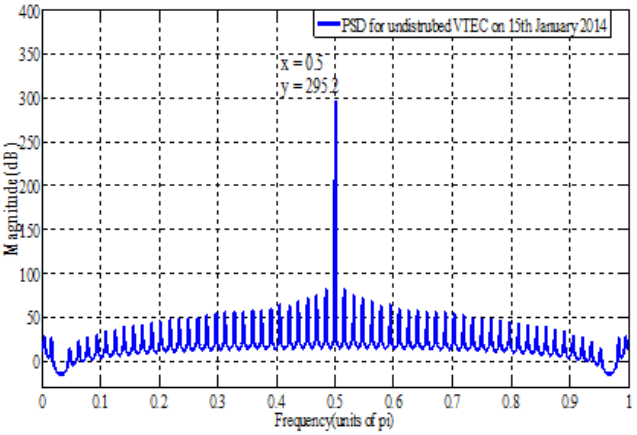

Figure 13. PSD for detrended undisturbed VTEC of 16th January 2014 for PRN 18.

Table 1. PSDs for detrended disturbed and Three consecutive days taking the earthquake day days taking the earthquake as the middle one

S. No.	Day of the year	PSD of disturbed VTEC	PSD of undisturbed VTEC
1	14th January 2014	315.6dB	299.5dB
2	15th January 2014	325.1dB	295.2dB
3	16th January 2014	309.5dB	287.1dB

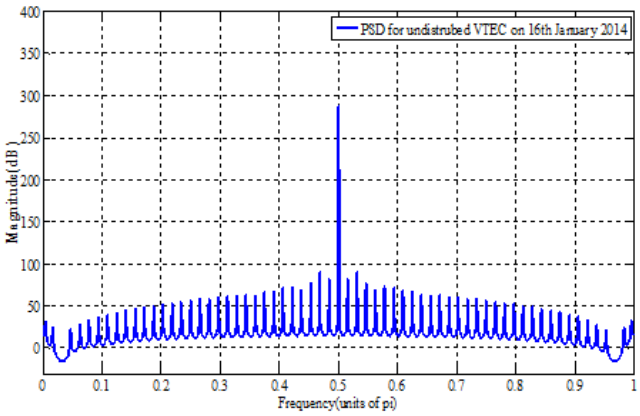

Figure 14. PSD for detrended undisturbed VTEC of 15th January 2014 for PRN 18.

The increase in PSD on the occurrence of the earthquake day is plotted in Figure 15. It is clearly observed that there is a significant raise in energy of the ionosphere on the day of earthquake occurrence.

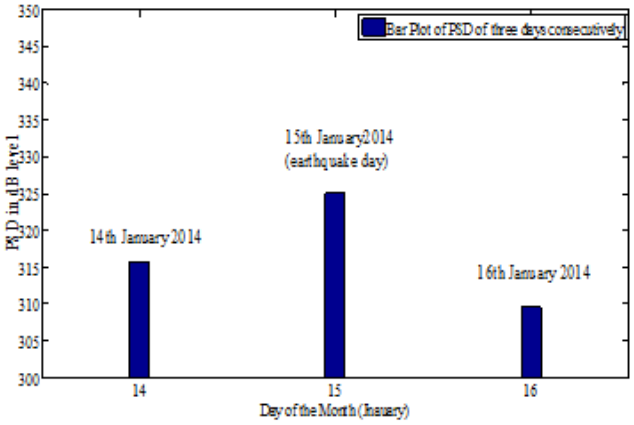

Figure 15. Histogram plot of the raise in PSD's for the undisturbed VTEC for three consecutive as the middle one.

6. Conclusion

The analysis of VTEC using MUSIC method can detect anomalies in the ionosphere resulting from the earthquake. The energy and momentum are transferred from lower to upper atmosphere during earthquake occurrence. A detailed analysis of these perturbations leads to the development of the early warning systems in future for these unpredictable natural disasters, Earthquakes.

7. Acknowledgement

This research is supported by the Department of Science and Technology (DST), Government of India via sponsored projects SR/AS-04/WOS-A/2011 and SR/S4/AS-9/2012. The authors would like to thank the DST panel of Atmospheric Sciences and President, Koneru Lakshmaih Univeristy for their continuous support and encouragement.

8. References

1. Zhang X, Shen X, Parrot M, Zeren Z, Ouyang X, Liu J, Qian J, Zhao S, Miao Y. Phenomena of electrostatic perturbations before strong earthquakes (2005–2010) observed on Demeter. Natural of Hazards Earth Systems Sciences. 2012; 12:75–83.
2. Sorokin VM, et al. Electrodynamic Model of the Lower Atmosphere and the Ionosphere Coupling. Journal of Atmospheric and Solar-Terrestrial Physics. 2001; 63:1681–91.
3. Pulinets S. Ionospheric Precursors of Earthquakes; Recent Advances in Theoryand Practical Applications. TAO. 2004; 15(3):413–35.
4. Lin JW. Ionospheric Total Electron Content (TEC) Anomalies Associated with Earthquakes through Karhunen-Loéve Transform (KLT). Terriestrial Atmosopheric Oceanic Sciences. 2010; 21(2):253–65.
5. Gosh D, Midy SK. Associating an ionospheric parameter with major earthquake occurrence throughout the world. Journal of Earth Systems and Science. 2014; 123(1):63–71.
6. Pulinets SA, Boyarchuk KA, Hegai VV, Karelin AV. Conception and model of seismo-ionosphere-magnetosphere coupling. In: Hayakawa M, Molchanov OA, editors. Seismo-Electromagnetics: Lithosphere-Atmosphere-Ionosphere Coupling, Terrapub, Tokyo; 2002. pp. 353–61.
7. Pulinets SA, Legenka AD, Alekseev VA. Pre-Earthquake Ionospheric Effects and their Possible Mechanisms, Dusty and Dirty Plasmas, Noise and Chaos in Space and in the Laboratory. New York: Plenum Press; 1994.
8. Mishra P, Enge P. Global Positioning Systems. 2nd ed. USA: Ganga-Jamuna Press; 2011.
9. Su YC, Liu JY, Chen SP, Tsai HF, Chen MQ. Temporal and spatial precursors in ionospheric total electron content of the 16 October 1999 Mw7.1 Hector Mine earthquake. Journal of Geophysical Research: Space Physics. 2013; 118(10):6511–7.
10. He LM, et al. Is there a One-to-One Correspondence Between Ionospheric Anomalies and Large Earthquakes along Longmenshan Faults?, Ann. Geophys. 2014; 32:187–96.
11. Lin JW. Ionospheric Precursor for the 20 April, 2013, M_w = 6.6 China' Lushan Earthquake: Two-Dimensional Principal Component Analysis (2DPCA). German Journal of Earth Sciences Research (GJESR). 2013; 1(1):1–12.
12. Jagan OLB, Rao KS, Jawahar A, Karishma SKB. Application of Particle Filter using Bearing Measurements. Indian Journal of Science and Technology. 2016; 9(7):1–4.
13. Jawahar A, Rao KS. Recursive Multistage Estimator for Bearings only Passive Target Tracking in ESM EW Systems. Indian Journal of Science and Technology. 2015; 8(26):1–5.
14. Annabattula J, Rao KS, Murthy SDA, Srikanth KS, Das PR. Multi-Sensor Submarine Surveillance System using MG-BEKF. Indian Journal of Science and Technology. 2015; 8(35):1–5.
15. Santhosh NM, Rao KS, Das RP, Raju L. Underwater Target Tracking using Unscented Kalman Filter. Indian Journal of Science and Technology. 2015; 8(31):1–5.
16. Hayes MH. Statistical Digital Processing and Modelling. USA: Georgia Institute of Technology, John Wiley and Sons, Inc; 1996.